Postprint of: Czaja Z., A microcontroller system for measurement of three independent components in impedance sensors using a single square pulse, Sensors and Actuators A: Physical, Vol. 173, Iss. 1 (2012), pp. 284-292, DOI: 10.1016/j.sna.2011.10.018

The microcontroller system for measurement of three independent components in impedance sensors using a single square pulse

Zbigniew Czaja*

Gdansk University of Technology, Faculty of Electronics, Telecommunications and Informatics, Department of Optoelectronics and Electronic Systems, ul. G. Narutowicza 11/12, 80-233 Gdansk, Poland

Abstract

A novel time domain method and its implementation in a simple smart impedance sensor controlled by an 8-bit microcontroller is presented in the paper. The method bases on stimulation of an impedance divider consisting of a resistor working as a voltage-to-current converter and the impedance sensor by a single square-voltage pulse with a duration time T directly generated by the output of the microcontroller and on sampling the resulting voltage on the sensor at three different selected moments $T/8$, $T/2$ and $7T/8$ by the internal ADC of the microcontroller. The sensor is modeled by a three-components circuit. The duration time T is determined by the first timer and the ADC is triggered by the second timer of the microcontroller. The measurement procedure is short and the determination of model component values bases on basic calculus. Thanks to this, smart sensors basing on this solution are energy-saving and low cost. Hence, they can be used in wireless sensor networks, especially basing on the ZigBee protocol. The results of the simulation investigation and the experimental verification of the method are included in this paper.

Keywords: Time-domain measurement, microcontroller interfacing, impedance sensors

1. Introduction

Electrical impedance-based sensors are usually modeled by two-terminal circuits consisting of several circuit components. Their models include a series or parallel combination of resistors R and capacitors C. Typically they consist of three e.g. for electrode–electrolyte systems with equal electrodes [1,2], capacitive RH sensors [3], for water conductivity measurements based on two electrodes [4,5], for pure titanium working electrodes immersed in phosphate buffered saline [6], five e.g. for electrode/bacteria /electrolyte interfaces for bacterial adhesion [7] and for single-crystalline silicon solar cells [8], six e.g. for fuel cells [9] or more components.

Component values of the impedance model of the sensors can be determined by using measurements in the frequency domain or in the time domain. In the first case we base on impedance spectroscopy, in the second case the current-time response of the sensor converted into the time-voltage response is sampled using a fast A/D and the FFT is performed [10,11] or this response is sampled three times and component values of the three-component model of the sensor are analytically calculated [1,2,4-6].

In impedance spectroscopy we stimulate the sensor using several sine waves with a wide spectrum of frequency values and we measure the resulting current or a voltage. This

* Corresponding author. Tel.: +48-58-347-1487; fax: +48-58-347-1357. *E-mail address:* zbczaja@pg.gda.pl

approach needs to apply a frequency impedance analyzer which consists of a generator with direct digital synthesis (DDS) and a vector voltmeter [12]. Hence, the measurement circuit is complex and it is not suitable for simple smart sensors, especially battery-powered and controlled by a microcontroller, and also working in wireless sensor networks, e.g. basing on the ZigBee protocol.

Also the time domain methods [10,11] are not appropriate for compact sensors systems. They base on FFT calculations which exact a big memory for data points and a powerful data processor, what increases a system cost. Additionally, the calculations lengthen the processor working time, what causes an increase of power consumption.

The methods reported in [1,2] are free from these disadvantages. In these methods three independent components of the impedance of a sensor are analytically determined by applying a single square-wave current [1] or a voltage [2] and measuring the resulting voltage [1] or the resulting current intensity [2] at only three different selected times.

Basing on an idea of these methods [1,2] and also on solutions from fault diagnosis methods of analog circuits elaborated by the author [13-15] the new method of measurement and analytical determination of three independent components of the impedance of a sensor was elaborated.

Thus, the paper describes this novel method and its implementation in a simple smart sensor controlled by a microcontroller. The method bases on stimulation of an voltage divisor consisting of a resistor working as a voltage-to-current converter (VTCC resistor) and the sensor (Fig. 1) by a single square voltage pulse and on sampling the resulting voltage on the sensor at three different selected moments. Because the impedance model is known, the values of three model components are calculated from three measurement results. The electronic circuit is simple. It consists of only the microcontroller (exactly: its internal devices: two timers and an ADC) and the VTCC resistor. The first timer determines the duration time of the single square pulse directly generated by the output of the microcontroller, and the voltage response is sampled by the ADC triggered by the second timer. If we need measurement results with a better voltage resolution, we have to add an external ADC to the system. Determination of model component values bases on basic calculus, which can be made with success by 8-bit microcontrollers.

2. Description of the method

The method consists of two parts: the measurement part, where the sensor is stimulated by a single square pulse, its voltage time response is sampled three times, and the calculation part in which the measurement result is used to analytical computations of components values of the sensor model.

It is assumed that the sensor is modeled by a three-component circuit consisting of a resistance R_{sp} connected in series with parallel connection of a resistance R_p and a capacitance C_p (Fig. 1) according to rules described in [2,4-6]. Nominal values of model components are the following: $R_{sp} = 100\ \Omega$, $R_p = 1000\ \Omega$, $C_p = 1\ \mu F$. These values were used for a simulation analysis and an experimental verification of the method. They are the same as in the template model in [2] what allows a better estimation of the proposed method.

On the current stage of investigations of the method, which results are presented in the paper, it has been resigned from the sensor model basing on a constant-phase element (CPE). It follows from the facts that it needs considerably more calculations to determine component values as presented in [1], what is inconvenience for systems controlled by 8-bit microcontrollers, or it is necessary extension of the method about analysis in the frequency domain to determine the CPE frequency dispersion factor [6].

2.1. The measurement circuits

The measurement circuit shown in Fig. 1 is composed from the VTCC resistor R_r connected in series with the impedance sensor Z_s (R_{sp} + $R_p \parallel C_p$). They create a voltage divider. The circuit is stimulated by a single square pulse v_{in} with an amplitude set a priori to V_{CC} (a supply voltage of the digital circuit (e.g. V_{CC} = 5 V) – the "Hi" level for digital signals). We measure the output voltage v_{out} on the sensor Z_s.

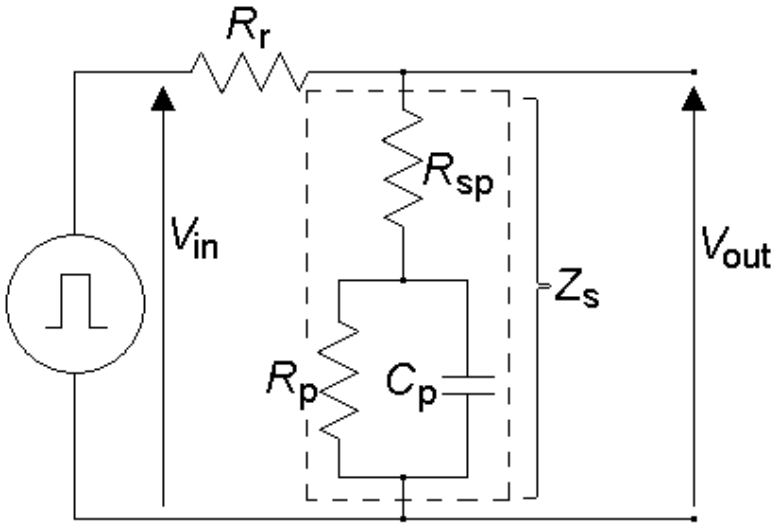

Fig. 1. Scheme of the measurement circuit

Hence, we can say that the ~~reference~~ VTCC resistor R_r works as a current-to-voltage converter, what is presented by the following formula:

$$v_{out} = v_{in} - i(R_{sp}, R_p, C_p)R_r \tag{1}$$

Thanks to this solution, we can treat the measurement circuit as a four-terminal circuit and therefore we can adapt ideas from fault diagnosis methods of analog circuits [13-15] for determination of components values of the impedance sensor model.

2.2. Circuit analysis

The measurement circuit is stimulated by a single square pulse with the duration time T (Fig. 2). It is assumed that the output signal $v_{out}(t)$ is sampled by an ADC at three moments as shown in Fig.2. Hence, we obtain following voltage samples: V_k, V_l, V_m. After normalization (after division of these values by V_{CC}) we obtain: $v_k = V_k / V_{CC}$, $v_l = V_l / V_{CC}$, $v_m = V_m / V_{CC}$.

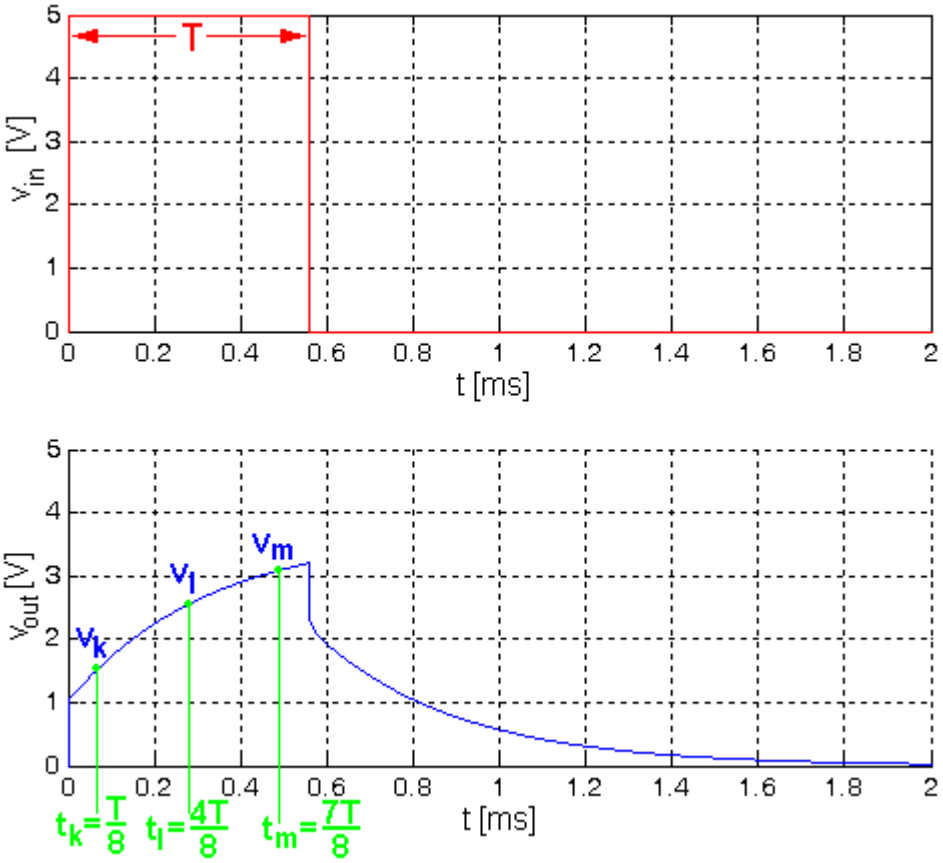

Fig. 2. Timings of the stimulation signal of the measurement circuits and the voltage time response of the impedance sensor

If we assume that

$$p = \frac{v_m - v_k}{v_k - v_l} \quad \text{and} \quad q = \frac{v_l - v_m}{v_k - v_l} \tag{2}$$

We can simplified (A.15) (see Appendix A) to the following form:

$$\rho^m + p\rho^l + q\rho^k = 0 \tag{3}$$

From (3) it is seen that it is important to set values k, l, m for which the equation is analytically resolvable. It is possible e.g. when $n = 8$ and $k = 1$, $l = 4$, $m = 7$. For these values (3) can be written as:

$$\rho^7 + p\rho^4 + q\rho = 0 \tag{4}$$

what gives:

$$\rho^6 + p\rho^3 + q = 0 \tag{5}$$

If we assume that $x = \rho^3$ we obtain from (5) the square equation:

$$x^2 + px + q = 0 \tag{6}$$

Its solution giving good results is

$$x = \frac{-p - \sqrt{p^2 - 4q}}{2} \tag{7}$$

Hence $\rho = \sqrt[3]{x}$. Because $\rho = e^{-\alpha \cdot \tau} = e^{-\alpha \cdot \frac{T}{n}}$ the α is calculated from:

$$\alpha = -\frac{n}{T} \ln \rho \tag{8}$$

Assuming that $\rho_k = \rho^k$ and $\rho_l = \rho^l$ we can transform (A.9) to the form:

$$\begin{cases} v_k = \vartheta + \delta \rho_k \\ v_l = \vartheta + \delta \rho_l \end{cases} \tag{9}$$

After derivations of (9) we have:

$$\vartheta = \frac{v_k \rho_l - v_l \rho_k}{\rho_l - \rho_k} \tag{10a}$$

$$\beta = \frac{v_k (\rho_l - 1) - v_l (\rho_k - 1)}{\rho_l - \rho_k} \tag{10b}$$

Therefore, we calculate the values of model components of the impedance sensor R_{sp}, R_p, C_p basing on these indirect parameters α, β, ϑ:

$$R_{sp} = R_r \frac{\beta}{1 - \beta} \tag{11a}$$

$$R_p = R_r \left(\frac{\vartheta}{1 - \vartheta} - \frac{\beta}{1 - \beta} \right) \tag{11b}$$

$$C_p = \frac{\frac{1}{1 - \vartheta}}{\alpha R_r \left(\frac{\vartheta}{1 - \vartheta} - \frac{\beta}{1 - \beta} \right) \frac{1}{1 - \beta}} \tag{11c}$$

We have got v_k, v_l, v_m values of voltage samples after the measurement part. Thus, to determine the R_{sp}, R_p, C_p component values we first have to calculate p and q values from (2), next we solve (7) and determine the ρ value and we compute indirect parameters α from (8), ϑ from (10a) and β from (10b), which are put into final formulas (11a) for R_{sp}, (11b) for R_p and (11c) for C_p. Hence, these calculations are not more complex, thanks to this they can be realized by 8-bit microcontrollers. E.g. the ATmega16 running with a 4 MHz quartz crystal oscillator needs about 8 ms to execute these calculations.

2.3. The microcontroller system

The laboratory microcontroller system for measurement of three independent components in impedance sensors is built with only the ATmega16 microcontroller of Atmel [16]. We decided to use the microcontroller with the AVR core, because Atmel offers compact 802.15.4/ZigBee modules with the ATmega1281 microcontroller and also the ATmega128RFA1 microcontroller family used in the 2.4GHz RF transceiver.

Thanks to this, the approach presented in the paper can be implemented directly in wireless sensor networks. It is sufficient to connect the impedance sensor to the ZigBee module (to appropriate pins of the microcontroller), obviously if it is required, via the conditioning circuit to assure good levels of stimulation and response signals, and to add functions serving the impedance sensors (realizing measurement and calculation procedures) to the ZigBee stack application layer. In other words, the proposed method allows to extend the functionality of the existing wireless module without its extension with electronic circuits. In this way, we obtain a small and compact wireless smart sensor.

As was mentioned above, to test the method and its possibilities, the laboratory microcontroller system based on the ATmega16 microcontroller (Fig. 3) was realized.

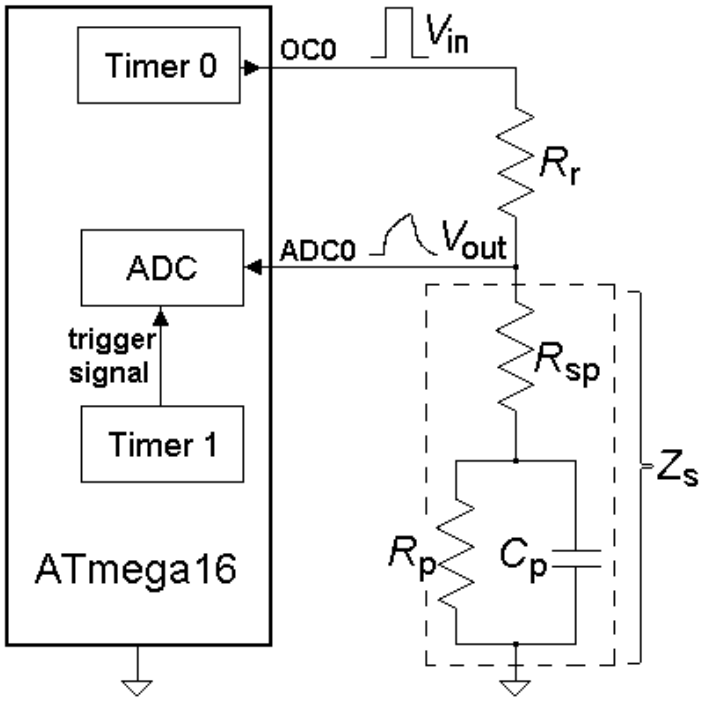

Fig. 3. The microcontroller system for testing of a impedance sensor

The measurement circuit is directly connected to the microcontroller pins. The stimulating square pulse is generated on the OC0 pin. Its duration time T is determined by the 8-bit Timer 0 working in the Compare Match Output Mode. The voltage response of the impedance sensor applied to the ADC0 pin is sampled three times by the 10-bit ADC, which is triggered by the 16-bit Timer 1 operating in the Clear Timer in Compare Match (CTC) Mode.

The measurement procedure is realized by the *measurement*() function. It consists of four code sections. The code placed in the main body of the function is responsible for initializing timers and the ADC, setting '1' on the OC0 output, starts the Timer 0 with the value corresponding to the duration time T and the Timer 1 with the value equivalent to $T/8$. The interrupt service of the Timer 0 hardware sets '0' on the OC0 output and stops the Timer 0. The interrupt of the Timer 1 hardware triggers the ADC conversion and writes in the next value to the Timer 1 representing $4T/8$ (the first interrupt activation) or $7T/8$ (the second one), or stops (the third one) the Timer 1. The first interrupt service of the ADC saves the 10-bit

conversion result in the variable *v_k*, the second one in the variable *v_l*, and the third one in the variable *v_m* and set the flag *end_measurement* used by the main function to finish the measurement procedure.

If there is any DC voltage V_{DC} existing on the impedance sensor, due for example to an electrode polarization, we can measure it before beginning of the measurement procedure. After execution of this procedure we should correct the measurement results by addition or subtraction V_{DC} to/from them. The measurement of V_{DC} is simple. We set the OC0 pin of the microcontroller as a high impedance input and next we measure the voltage V_{DC} on the ADC0 pin by the ADC. But, we should remember that in this case, a limitation of the method is fact that $V_m + V_{DC} \leq V_{CC}$.

2.4. Selection of the duration time T and the value of the VTCC resistor R_r

To obtain the best measurement resolution it is important to determine optimum values of the duration time T and the VTCC resistor R_r. We know the nominal values of three components of the impedance sensor model. Hence, we have to assume ranges of changes of their values. They depend on the impedance sensor type and on the working environment. In the paper, for illustration of this analysis we assume that all component values change from 0.1 to 10 times their nominal value.

It is seen from (2) that we have to analyze differences between voltage samples: $v_l - v_k$, $v_m - v_l$ and $v_m - v_k$ in a function of T and R_r. From timing of the voltage time response of the impedance sensor (Fig. 2) we can observe that $v_m - v_l < v_l - v_k < v_m - v_k$. Hence, it is enough to analyze only the smallest difference $v_{ml} = v_m - v_l$.

The ζ_i coefficient of the i-th component (where i = 1 (R_{sp}), 2 (R_p), 3 (C_p)) in a function of changes of T values and R_r values is introduced:

$$\zeta_i(T, R_r) = \max_{p_i \in \langle p_{i\min}, p_{i\max} \rangle} \{v_{ml}(p_i, T, R_r)\} - \min_{p_i \in \langle p_{i\min}, p_{i\max} \rangle} \{v_{ml}(p_i, T, R_r)\} \tag{12}$$

where p_i – the value of the i-th component in a range from $p_{i\,min} = 0.1 p_{i\,nom}$ to $p_{i\,max} = 10 p_{i\,nom}$ ($p_{i\,nom}$ - the nominal value of the i-th component), $v_{ml}(p_i, T, R_r)$ – the v_{ml} value in a function of changes of p_i component values, T values and Rr values.

Therefore, the ζ_i coefficient is defined as the difference between maximum and minimum values v_{ml} computed for an assumed range of changes of p_i component values for particular values of T and R_r. Other words, the ζ_i coefficient value informs us about the range of changes of v_{ml} values, that is we can say about dynamics of these changes, for given values of T and R_r in the function of changes of the p_i component values. If the ζ_i value is the greatest, the increased sensitivity of the voltage transmittance ~~transfer function~~ of the measurement circuit to deviations of values of the i-th component is also the biggest. That is we obtain possibly the best measurement conditions. Thanks to this, we can optimally increase the resolution threshold of the value component determination. Graphs of ζ_i coefficients for respective components in a function of T and R_r are shown in Fig. 4. Hence, we have to determine the maximum value $\zeta_{i\,max}$ from the ζ_i values set (drawn in Fig. 4) calculating for value changes of T and R_r. $\zeta_{i\,max}$ points to optimum values of $T_{i\,opt}$ and $R_{r\,i\,opt}$:

$$\zeta_{i\max} = \max_{R_r \in \langle R_{r\min}, R_{r\max} \rangle} \left\{ \max_{T \in \langle T_{\min}, T_{\max} \rangle} \{\zeta_i(T, R_r)\} \right\} \rightarrow R_{r\,i\,opt}, T_{i\,opt} \tag{13}$$

where we assumed that $R_{r\,min} = R_{sp}$, $R_{r\,max} = R_p$, $T_{min} = 0.1 R_{sp} C_p$, $T_{max} = 3 R_{sp} C_p$.

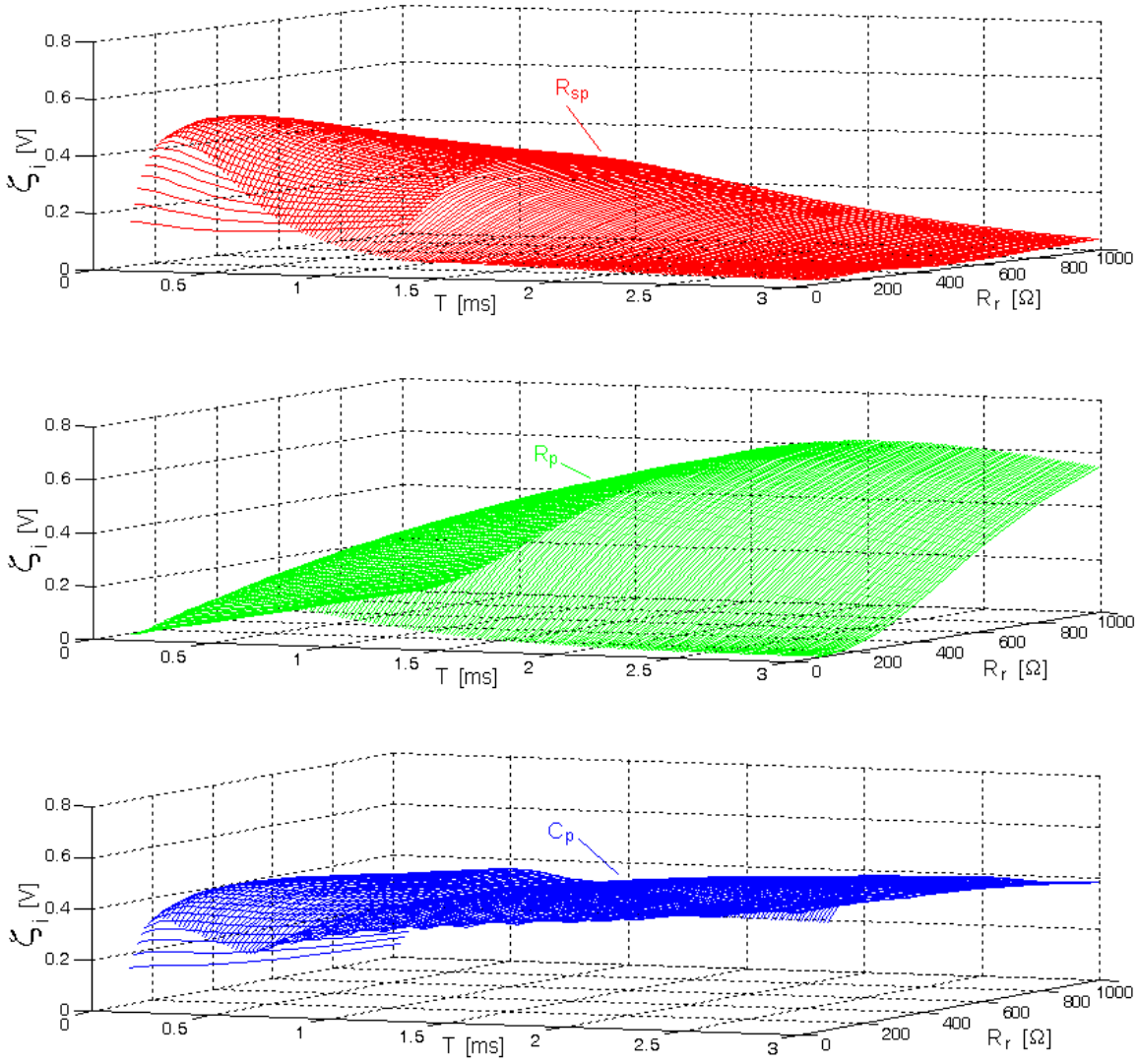

Fig. 4. The ζ_i coefficients in the function of T and R_r for R_{sp}, R_p, C_p, respectively

Obviously, the Eq. (13) allows to determine the best measurement conditions for one i-th component. E.g. if we want to optimize the measurement condition for chosen two components or for all components it is proposed to use an average value denoted as ζ of ζ_i coefficients of considered components:

$$\zeta(T,R_r)=\frac{1}{I}\sum_{i=1}^{I}\zeta_i(T,R_r) \tag{14}$$

where $I = 2$ – if we chose two components, or $I = 3$ – if we chose all components.

The ζ coefficient for $I = 3$ is illustrated in Fig. 5. In this case, we also find its maximum value which points to optimum values of $T_{i\,opt}$ and $R_{r\,i\,opt}$.

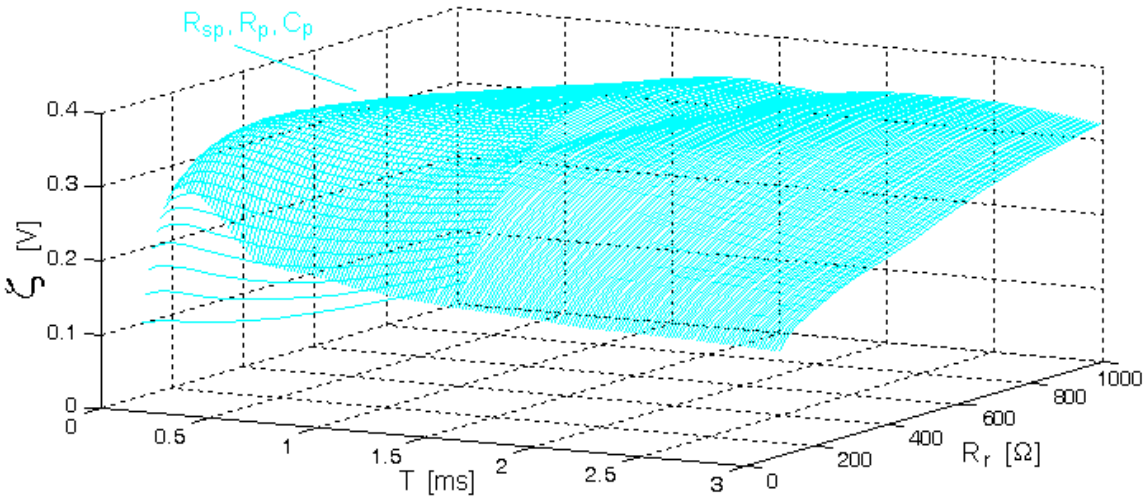

Fig. 5. The average value of ζ_i coefficients in the function of T and R_r for all components: R_{sp}, R_p, C_p

All determined results of optimum values of $T_{i\ opt}$ and $R_{r\ i\ opt}$ are included in Table 1. To analyze we use values of $R_{r\ i\ opt}$ taken from the E12 series of standard values of the IEC-63 Standard. Thanks to this, the VTCC resistor R_r consists of one generally available element, what simplifies the measurement circuit and reduces implementation costs.

Table 1. Optimum values of $T_{i\ opt}$ and $R_{r\ i\ opt}$ assuring the best measurement conditions

Investigated component	$T_{i\ opt}$ **[ms]**	$R_{r\ i\ opt}$ **[Ω]**
R_{sp}	0.32	220
R_p	2.08	1000
C_p	3.00	330
R_{sp}, R_p, C_p	0.56	390

To analyze we chose $T_{i\ opt}$ = 0.56 ms and $R_{r\ i\ opt}$ = 390 Ω assuring possibly the best measurement conditions for all components of the impedance sensor model.

3. Experimental results

The main aim of experimental investigations was examination of metrological possibilities of the microcontroller system built with only the microcontroller (in our case the ATmega16) and its internal devices (timers and the ADC). Hence, the new method was experimentally verified and estimated on the example of a physical model built according to the scheme shown in Fig. 1. The model with known values of its components allowed to compare these values with those appointed by the method with theoretical ones (physically set in the circuit). Thanks to this, it was possible to estimate the measurement resolution of the microcontroller system and relate it with the precision of determination of model component values.

The measurement part of the microcontroller system consists of the VTCC resistor R_r = 389.9 Ω, and the physical model of the impedance sensor assembled with two resistors with nominal values R_{sp} = 100.18 Ω, R_p = 1000.2 Ω and one capacitor with the nominal value C_p = 1.016 μF. The digital part is represented by the Atmega16 16PI 0509J, which runs with a 4 MHz quartz crystal oscillator. The Timer 1 is clocked directly by the system clock. It is

used to determine the voltage sample moments t_k= 70 μs, t_l= 280 μs and t_m= 490 μs. The Timer 0 works in the Compare Match Output Mode with the toggle mode of the OC0 output and it is clocked by the system clock with the prescaler divisor 64. It generates at the output OC0 a stimulating square pulse with the duration time T = 560 μs and with an amplitude equal to V_{CC} = 5.2106 V. Resistance and voltage values were verified with the HP34401A multimeter and capacitance values by the 4263B LCR meter at 1 kHz frequency.

After preliminary investigations it was proved that electrical parameters (especially the output pin impedance depending on the pin sink current [16]) of the OC0 output pin of the microcontroller, as also affirmed in [3,17,18], considerably influence the divergence between measurement results and simulation results. To eliminate this influence an inverter built from one IRF7105 component was added on the OC0 output (Fig. 6). The IRF7105 consists of two HEXFET power MOSFETs, the first one with a N-channel and the second one with a P-channel [19]. Additionally, small values of static drain-to-source on-resistances (0.1 Ω and 0.25 Ω for N-channel and P-channel transistors respectively) and big values of continuous drain currents (3.5 A and –2.3 A adequately) allow to extend the measurement range of the system.

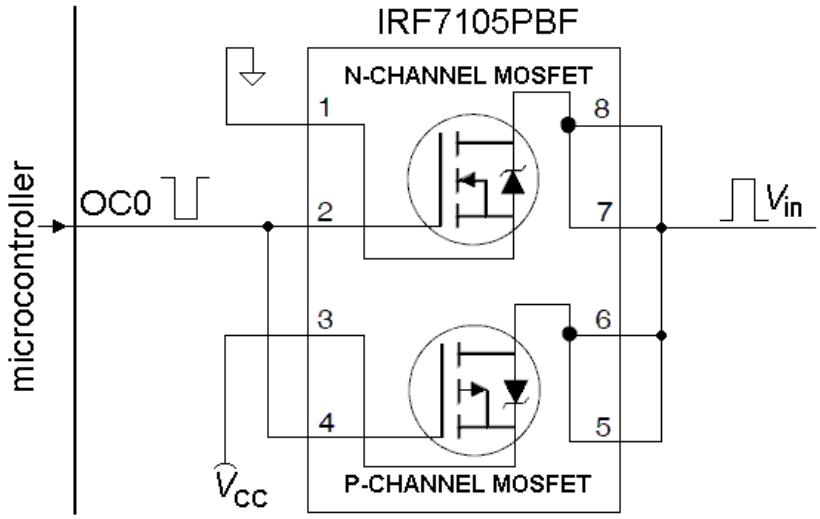

Fig. 6. The inverter basing on the IRF7105 introduced between the OC0 output of the microcontroller and the sensor

For the considered laboratory system the average consumption of the supply current during the measurement procedure was measured. Its value is equal to 21.5 mA. We should remember that to estimate the energy consumption it is necessary to consider yet the ADC conversion time lengthening the measurement procedure. For the assumed 10-bit resolution and the ±2 LSB absolute accuracy [16] of the ADC (the input clock frequency is set to 125 kHz) this time is equal to about 104 μs.

Measurements were carried out for 33 values of each model component by making the assumption that remaining component values are constant. The values were logarithmically located in the following ranges of component value changes: from 10 Ω to 1 kΩ for the R_{sp} resistor, from 100 Ω to 10 kΩ for the R_p resistor and from 100 nF to 10 μF for the C_p capacitor. Three voltage samples v_k, v_l and v_m were measured by the 10-bit ADC of the microcontroller. Measurement results of voltages and determined values of model components were stored with 16-bit resolution (using integer type variables) and sent to a personal computer via the RS232 interface.

Considering (2) it is seen that in fact values of differences between respective voltage samples have an essential impact on the determination of values of sensor model components.

Hence, these values are taken into account. Their graphs in a function of changes of values of respective components are drawn in Fig. 7. The measurement results are marked by circles for $v_{kl} = v_k - v_l$, squares for $v_{lm} = v_l - v_m$ and triangles for $v_{mk} = v_m - v_k$. Continuous lines represent simulation results. Values of voltages are expressed in the form of values directly read from the 10-bit ADC (the number of LSBs).

Comparing the experimental results with theoretical ones it is seen that measurements are convergent with the simulation results, what testifies correct operation of the measurement procedure and the microcontroller hardware.

Maximum ranges of value deviations between experimental and simulation results (measurement absolute errors) for complete ranges of component value changes are presented in Table 2.

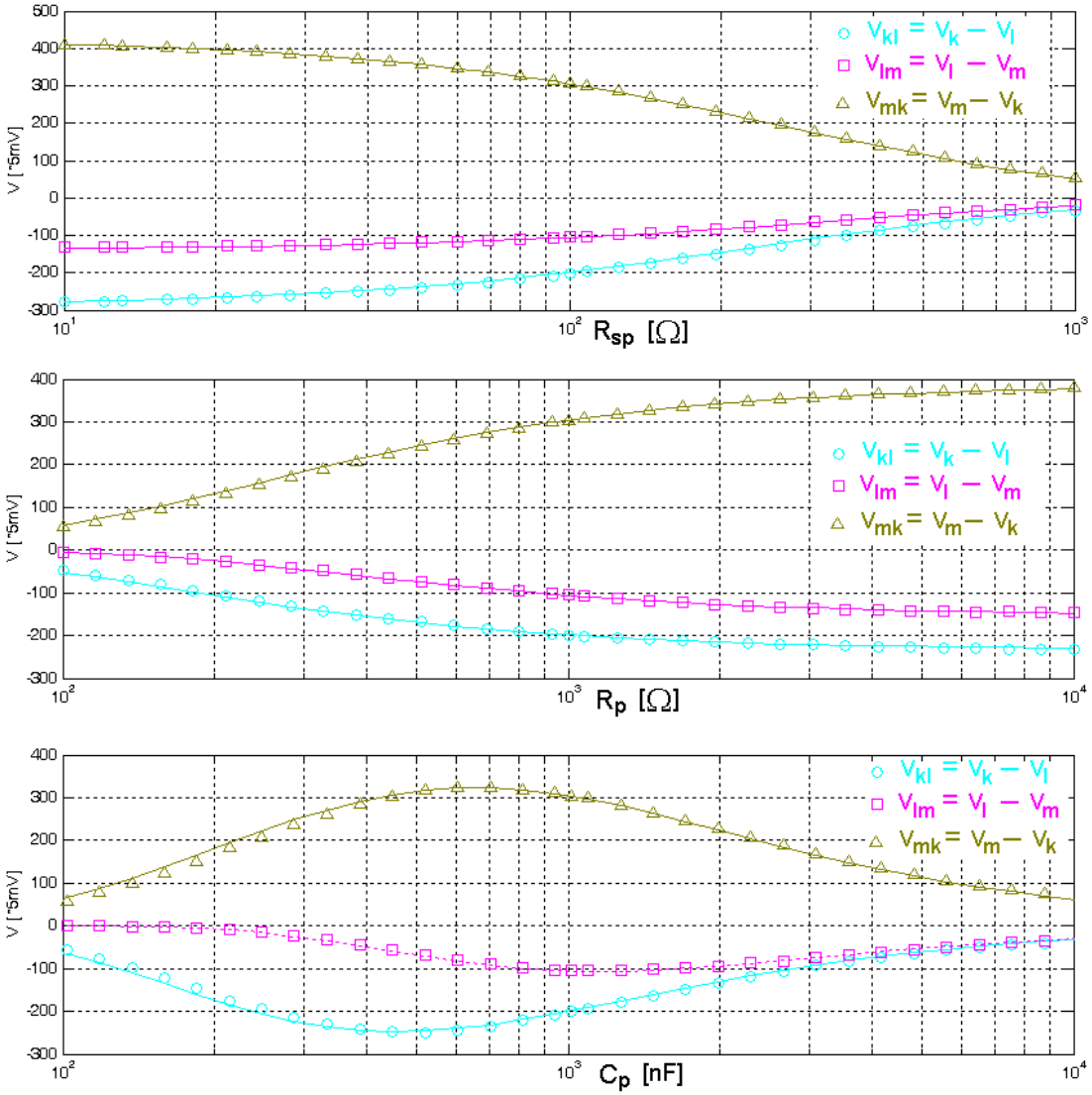

Fig. 7. Graphs of measurement results represented by values of differences between respective voltage samples: $v_{kl} = v_k - v_l$, $v_{lm} = v_l - v_m$, $v_{mk} = v_m - v_k$.

Except absolute errors appointed for the C_p component value changes all remaining absolute errors are comprised in the range of the absolute uncertainty of the 10-bit ADC triggered by the 16-bit Timer. The value of this uncertainty depends on the absolute accuracy of the ADC [16], the uncertainty in microcontroller-based time measurements [20,21] and the uncertainty resulting from the method of start the ADC conversion [16,22] (impossibility of

synchronization of a prescaler clock signal of the ADC by the timers). From [22] it follows that the uncertainty of a single voltage measurement is about on the level equal to ±3 LSB. Hence, we can assume that the uncertainty of determination of difference between two voltage samples is on the level ±5 LSB. The big values of absolute errors determined for the C_p follow from the fact that for small values of capacitances optimum measurement conditions are not fulfilled (the C_p capacitor is too quickly charged, what causes that e.g. $v_l = v_m$, therefore the established value of the duration time T is too long for this case).

Table 2. Maximum ranges of changes of absolute measurement errors for complete ranges of component value changes

absolute error **component**	Δv_{kl} [*5 mV]	Δv_{lm} [*5 mV]	Δv_{mk} [*5 mV]
$\boldsymbol{R_{sp}}$	1 - 6	-3 - 0	-5 - 1
$\boldsymbol{R_p}$	-6 - 5	-3 - 1	-3 - 6
$\boldsymbol{C_p}$	-14 - 6	-3 - 2	-7 - 14

4. Determination of component values

Relative errors of the component values determined from measurement results for changes of values of respective components are plotted on Fig. 8, where $R_{sp\,nom}$, $R_{p\,nom}$ and $C_{p\,nom}$ represent nominal values of R_{sp}, R_p and C_p components respectively.

Obviously, these errors directly follow from measurement errors. However, apart from values of the measurement errors, the bad (even very bad) numerical conditions of component determination formulas have an essential influence on their big values. Particularly, it is seen that for (2) the measurement errors significantly accumulate themselves in the case of small values of v_{kl} (we should remember about the 10-bit measurement resolution), and next, formula (8) "amplifies" them. This effect is shown in Table 3. It presents simulation results basing on the Monte Carlo method [23] of relative uncertainties of component determination as a function of a measurement uncertainty. A rectangular probability distribution function (pdf) of the measurement uncertainty was assumed and a 99.73 % coverage interval of the uncertainties of the components determination.

Table 3. Relative uncertainties of components determination as a function of a measurement uncertainty

Measurement absolute (relative) uncertainty	**Relative uncertainty of values components determination**		
	δ_{Rsp} [%]	δ_{Rp} [%]	δ_{Cp} [%]
±2 LSB for 16-bit ADC (δ_{meas} = 0.0031%)	0.032	0.12	0.04
±2 LSB for 14-bit ADC (δ_{meas} = 0.012%)	0.13	0.48	0.16
±2 LSB for 12-bit ADC (δ_{meas} = 0.05%)	0.51	1.91	0.64
±2 LSB for 10-bit ADC (δ_{meas} = 0.2%)	2	7.6	2.55
±4 LSB for 10-bit ADC (δ_{meas} = 0.4%)	4.01	15.16	5.06

From Table 3 it is seen that the values of relative uncertainties of component determination for R_{sp} (δ_{Rsp}), R_p (δ_{Rp}) and C_p (δ_{Cp}) are about 10 times, 38 times and 13 times higher than the measurement uncertainty (δ_{meas}) respectively. Unfortunately, this disadvantage follows from the fact that the proposed method belongs to a class of time domain methods.

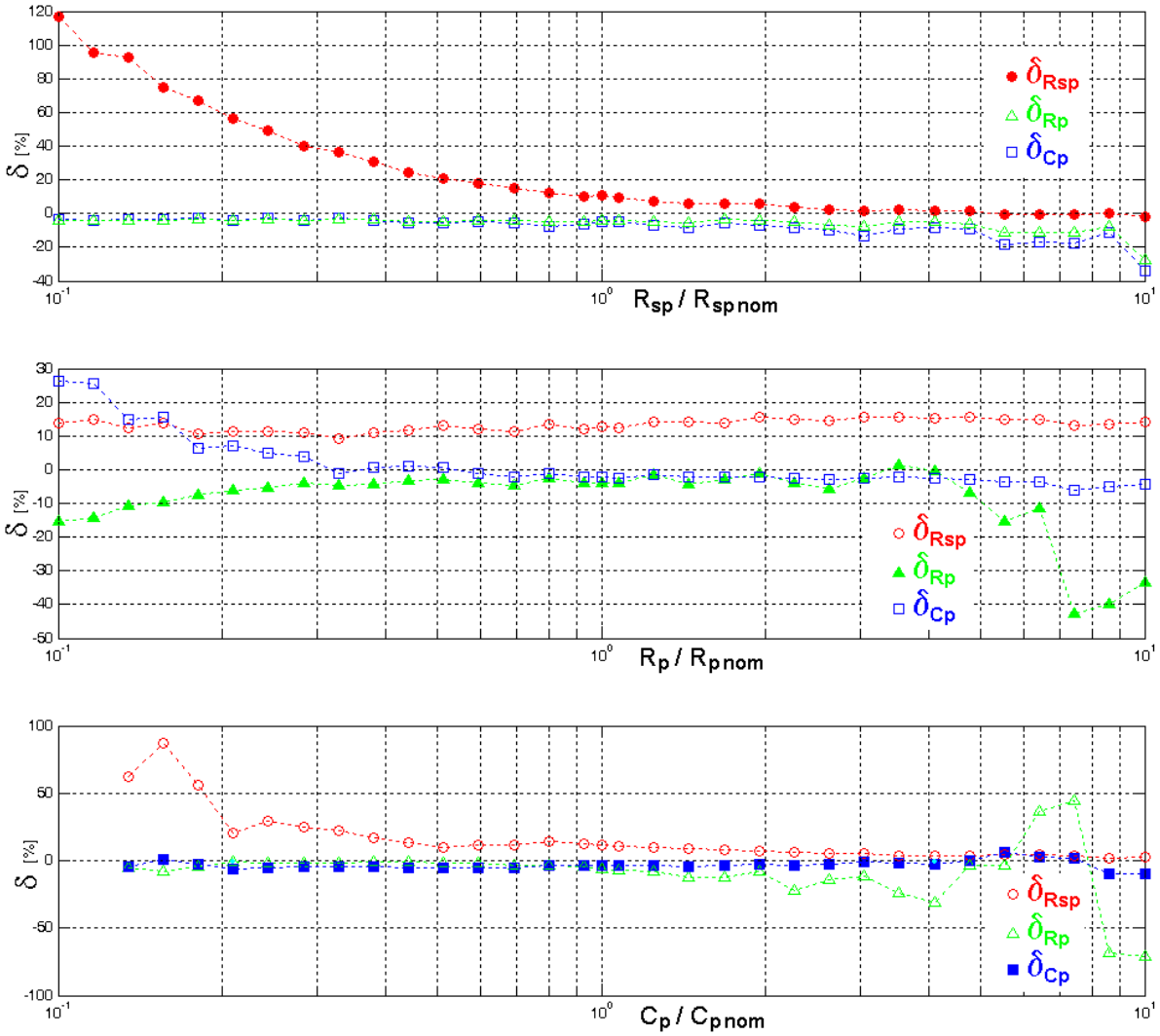

Fig. 8. Graphs of relative errors of component value determination from measurement results

The described feature of the method is particularly visible for the relative errors δ_{Rsp} (Fig. 8) of the R_{sp} value component determination. For relatively constant values of absolute measurement errors (Fig. 7) and more and more smaller values of the R_{sp} component (more and more smaller an impact of the R_{sp} component on the sensor impedance) set during the measurements, the relative error δ_{Rsp} grows and for $R_{sp} = 10\ \Omega$ achieves even 120 % (the graph δ_{Rsp} as a function of $R_{sp} / R_{sp\ nom}$).

Around nominal values of sensor model components the relative errors of the values of component determination are similar to uncertainties corresponding to them presented in Table 3, what confirms that measurements were made for the best possible measurement conditions. These conditions are not optimal for extreme values of the components, what leads to effective growth of the relative errors. Moreover, the numerical conditions cause that e.g. for two the smallest values of the C_p component, for which $v_l = v_m$, the formula (8) is incomputable.

The described problems follow from the fact that we have taken restrictive assumptions for investigations of the microcontroller measurement system. That is, we assumed a very wide range of value changes for all components of the sensor model and we have set one optimum value of the duration time T and one optimum value of the VTCC resistor R_r for this range.

Summarizing we can affirm that the proposed microcontroller system for measurements of three independent components in impedance sensors using a single square pulse works properly according to the presented theory. The measurements characterize an unusually big repeatability as for this hardware, what was exactly tested. The experimental results confirm that an advantage of the presented time domain method (very short time of measurements) is simultaneously its disadvantage (small accuracy of determination of components values of the sensor model). Obviously, it is possible to improve this accuracy. Usually, in real applications changes of values of a given physical quantity have a predominant influence typically on values of one component of the sensor model. Thus, it allows to match the best measurement conditions for this component and to change these conditions (e.g. the duration time T) according to expected values of this component. Moreover, changes of values of a given component can be presented in the form of identification curves [13-15] scaled directly in values of a given physical quantity (it allows to use a look-up technique), what eliminates firstly the calculations biased by the bad numerical conditions needed for component value determination and secondly the calculations converting these values to values of a given physical quantity.

5. Conclusion

In the paper a microcontroller system for measurement of three independent components in impedance sensors using a single square pulse and the new time domain method elaborated for this system are presented. The system is simple, because it consists only of the 8-bit microcontroller (exactly: its internal devices: two timers and the ADC), the inverter built from two MOSFETs and the VTCC resistor. The measurement procedure is short and determination of model components values bases on basic calculus. These advantages follow from the fact that the system was designed for simple small smart sensors, especially battery-powered and also working in wireless sensor networks, e.g. basing on the ZigBee protocol.

Thanks to this, smart sensors basing on this solution are energy-saving and low cost, what allows to implement them in large wireless sensor networks.

Obviously, there are methods [4-6] which need about ten times less calculations to determine component values from measurement results and they also characterize a smaller influence of measurement uncertainly on estimation of component values than the proposed method. But, their implementation on such simple systems is considerably more difficult. Their measurement procedure is complex, it takes more time and it requires complex calculations and storage the set of acquired measurement data. Additionally, there are high requirements on measurement conditions minimalizing the measurement errors, which can't be fulfilled by the ADC of the microcontroller.

As an analysis of uncertainties of components determination and experimental investigations proved, the proposed time domain method characterizes the small accuracy of the component value determination. Hence, with regard to its small accuracy and the advantages quoted above, the smart sensors basing on this method are ideally suitable for monitoring of physical objects, and testing that their parameters do not exceed the assumed threshold values. E.g. if threshold values are exceeded the smart sensor working as an endpoint of the wireless network can send this information to a network coordinator, who can

turn on an another type more advanced sensor basing on the more energy-consuming but more accurate frequency domain method.

Appendix A

The measurement circuit is stimulated by a single square pulse with the duration time T (Fig. 2). In the time domain this excitation can be described by the formula:

$$v_{in}(t) = V_{CC}\left(\mathbf{1}(t) - \mathbf{1}(t-T)\right) \tag{A.1}$$

Converting it to Laplace's domain, we obtain the form:

$$V_{in}(s) = V_{CC}\left(\frac{1}{s} - \frac{1}{s}e^{-sT}\right) \tag{A.2}$$

The measurement circuit can be treated as a four-terminal circuit (Fig. 1). Hence, its voltage transmittance can be written as:

$$K_u(s) = \frac{V_{out}(s)}{V_{in}(s)} = \frac{s\beta + \gamma}{s + \alpha} \tag{A.3}$$

where:

$$\alpha = \frac{R_r + R_{sp} + R_p}{C_p R_r R_p + C_p R_{sp} R_p} \tag{A.4.a}$$

$$\beta = \frac{C_p R_{sp} R_p}{C_p R_r R_p + C_p R_{sp} R_p} \tag{A.4.b}$$

$$\gamma = \frac{R_{sp} + R_p}{C_p R_r R_p + C_p R_{sp} R_p} \tag{A.4.c}$$

That is, the response signal $V_{out}(s)$ of the impedance sensor is the output signal of the four-terminal circuit (Fig. 1) what is expressed by:

$$V_{out}(s) = K_u(s)V_{in}(s) = V_{CC}\left(\frac{\beta}{s+\alpha} + \frac{\gamma}{s(s+\alpha)}\right). \tag{A.5}$$

After transformations in the time domain the output signal $v_{out}(t)$ has the form:

$$v_{out}(t) = \begin{cases} V_{CC}\left(\beta e^{-\alpha t} + \dfrac{\gamma}{\alpha}\left(1 - e^{-\alpha t}\right)\right) & \text{for } 0 \le t < T \\ V_{CC}\left(\beta - \dfrac{\gamma}{\alpha}\right)\left(e^{-\alpha t} - e^{-\alpha(t-T)}\right) & \text{for } t \ge T \end{cases} \tag{A.6}$$

if we assume $\vartheta = \dfrac{\gamma}{\alpha}$ that:

$$v_{out}(t) = \begin{cases} V_{CC}\left(\vartheta + (\beta - \vartheta)e^{-\alpha t}\right) \text{ for } 0 \le t < T \\ V_{CC}(\beta - \vartheta)\left(e^{-\alpha t} - e^{-\alpha(t-T)}\right) \text{ for } t \ge T \end{cases}. \tag{A.7}$$

It is assumed that the output signal $v_{out}(t)$ is sampled by an ADC at three moments: $k\tau$, $l\tau$, $m\tau$ and $\begin{cases} k,l,m,n \in \mathbf{N} \\ k < l < m \le n \end{cases}$ where $\tau = \frac{T}{n}$, and n is the number of the period T division. Hence, the voltage values for these moments are following: $V_k = v_{out}(k\tau)$, $V_l = v_{out}(l\tau)$, $V_m = v_{out}(m\tau)$. After normalization (after division of these values by V_{CC}) we obtain: $v_k = V_k / V_{CC}$, $v_l = V_l / V_{CC}$, $v_m = V_m / V_{CC}$. Thus, basing on (A.7) we derived formulas for v_k , v_l , v_m :

$$\begin{cases} v_k = \vartheta + (\beta - \vartheta)e^{-\alpha k\tau} \\ v_l = \vartheta + (\beta - \vartheta)e^{-\alpha l\tau} \\ v_m = \vartheta + (\beta - \vartheta)e^{-\alpha m\tau} \end{cases} \tag{A.8}$$

If we place $\delta = \beta - \vartheta$ and $\rho = \mathrm{e}^{-\alpha\tau}$ into (A.8), we obtain the following equations:

$$\begin{cases} v_k = \vartheta + \delta\rho^k \\ v_l = \vartheta + \delta\rho^l \\ v_m = \vartheta + \delta\rho^m \end{cases} \tag{A.9}$$

Subtracting the first equation from the second one of (A.9) we obtain:

$$v_l - v_k = \delta\left(\rho^l - \rho^k\right) \tag{A.10}$$

From (A.10) we determine:

$$\delta = \frac{v_l - v_k}{\rho^l - \rho^k} \tag{A.11}$$

This result we put to the third equation of (A.9) what gives:

$$v_m = \vartheta + \frac{v_l - v_k}{\rho^l - \rho^k}\rho^m \tag{A.12}$$

From (A.12) we assign ϑ:

$$\vartheta = v_m - \frac{v_l - v_k}{\rho^l - \rho^k}\rho^m \tag{A.13}$$

Next, the ϑ is put to the first equation of (A.9), what gives:

$$v_k = v_m - \frac{v_l - v_k}{\rho^l - \rho^k}\rho^m + \frac{v_l - v_k}{\rho^l - \rho^k}\rho^k \tag{A.14}$$

what after transformations gives the equation with only one unknown quantity ρ:

$$\rho^m + \rho^l \frac{v_m - v_k}{v_k - v_l} + \rho^k \frac{v_l - v_m}{v_k - v_l} = 0 \tag{A.15}$$

Formula (A.15) is used as a basis to next transformations made in the text.

References

[1] J. Lario-Garcia, R. Pallàs-Areny, Constant-phase element identification in conductivity sensors using a single square wave, Sensors and Actuators A 132 (2006) 122–128.

[2] J. Lario-Garcia, R. Pallàs-Areny, Measurement of three independent components in impedance sensors using a single square wave, Sensors and Actuators A 110 (2004) 164–170.

[3] F. Reverter, O. Casas, Direct interface circuit for capacitive humidity sensors, Sensors and Actuators A 143 (2008) 315–322.

[4] A. Mejía-Aguilar, R. Pallàs-Areny, Electrical impedance measurement using pulse excitation, Proceedings of 16th IMEKO TC4 Symposium, September 22 – 24, Florence, Italy (2008) 567-572.

[5] A. Mejía-Aguilar, R. Pallàs-Areny, Electrical impedance measurement using voltage/current pulse excitation, Proceedings of XIX IMEKO World Congress, September 7 – 11, Lisbon, Portugal (2009) 662-667.

[6] M. T.Ehrensberger, J. L.Gilbert, A time-based potential step analysis of electrochemical impedance incorporating a constant phase element: a study of commercially pure titanium in phosphate buffered saline, Journal of Biomedical Materials Research Part A 93 (2010) 576-584.

[7] S. Bayoudha, A. Othmane, L. Ponsonnet, H. B. Ouada, Electrical detection and characterization of bacterial adhesion using electrochemical impedance spectroscopy-based flow chamber, Colloids and Surfaces A: Physicochem. Eng. Aspects 318 (2008) 291–300.

[8] S. Kumar, P. K. Singh, G. S. Chilana, Study of silicon solar cell at different intensities of illumination and wavelengths using impedance spectroscopy, Solar Energy Materials & Solar Cells 93 (2009) 1881–1884.

[9] M. A. Danzer, E. P. Hofer, Electrochemical parameter identification—An efficient method for fuel cell impedance characterisation, Journal of Power Sources 183 (2008) 55–61.

[10] C. E. B. Neves, M. N. Souza, A method for bio-electrical impedance analysis based on a step-voltage response, Physiological Measurement 21 (2000) 395–408.

[11] A. R. Waterworth, P. Milnes, R. H. Smallwood, B. H. Brown, Cole equation modelling to measurements made using an impulse driven transfer impedance system, Physiol. Meas. 21 (2000) 137–144.

[12] J. Hoja, G. Lentka, Interface circuit for impedance sensors using two specialized single-chip microsystems, Sensors and Actuators A 163 (2010) 191–197.

[13] Z. Czaja, A diagnosis method of analog parts of mixed-signal systems controlled by microcontrollers, Measurement 40 (2007) 158-170.

[14] Z. Czaja, Using a square-wave signal for fault diagnosis of analog parts of mixed-signal electronic embedded systems, IEEE Transactions on Instrumentation and Measurement 57 (2008) 1589-1595.

[15] Z. Czaja, A method of fault diagnosis of analog parts of electronic embedded systems with tolerances, Measurement 42 (2009) 903-915.

[16] Atmel Corporation, 8-bit AVR microcontroller with 16k Bytes In-System Programmable Flash, ATmega16, ATmega16L, PDF file, (2003)
[17] F. Reverter, J. Jordana, M. Gasulla, R. Pallàs -Areny, Accuracy and resolution of direct resistive sensor-to-microcontroller interfaces, Sensors and Actuators A 121 (2005) 78–87.
[18] F. Reverter, O. Casas, Interfacing Differential Capacitive Sensors to Microcontrollers: A Direct Approach, IEEE Transactions on Instrumentation and Measurement, vol. 59, no. 10, (2010) 2763-2769.
[19] International Rectifier, IRF7105 HEXFET Power MOSFET, PDF file, (2003)
[20] F. Reverter, J. Jordana, R. Pallàs-Areny, Internal trigger errors in microcontroller-based measurements, Proceedings of XVII IMEKO World Congress, June 22 – 27, Dubrovnik, Croatia (2003) 655-658.
[21] F. Reverter, R. Pallàs -Areny, Uncertainty reduction techniques in microcontroller-based time measurements, Sensors and Actuators A 127 (2006) 74–79.
[22] Z. Czaja, Wykorzystanie przetworników A/C wbudowanych w mikrokontrolery do pomiarów parametrów sygnałów zmiennych (Using of internal ADCs of microcontrollers for measurements of alternating signal parameters), Przegląd Elektrotechniczny (Electrical Review) 86 (2010) 5 – 8.
[23] JCGM 101:2008, Evaluation of measurement data — Supplement 1 to the "Guide to the expression of uncertainty in measurement" — Propagation of distributions using a Monte Carlo method, JCGM 2008.